POLITECNICO DI TORINO Repository ISTITUZIONALE

A current transformer energy harvester with stable output based on the saturable magnetic core

Original A current transformer energy harvester with stable output based on the saturable magnetic core / Cao, Ja; Jiao, YI; Meng, Gf; Peng, J; Stassi, S; Pirri, F; Li, Yj In: ELECTRONICS LETTERS ISSN 0013-5194 ELETTRONICO 58:18(2022), pp. 705-707. [10.1049/ell2.12566]
Availability: This version is available at: 11583/2974498 since: 2023-01-11T09:51:22Z
Publisher: WILEY
Published DOI:10.1049/ell2.12566
Terms of use:
This article is made available under terms and conditions as specified in the corresponding bibliographic description in the repository
Publisher copyright

(Article begins on next page)

A current transformer energy harvester with stable output based on the saturable magnetic core

Jianan Cao,^{1,™} Yuanliang Jiao,¹ Gefei Meng,¹ Jia Peng,¹ Stefano Stassi,² Fabrizio Pirri,² and Yunjia Li¹

One of the major bottlenecks of the traditional current transformer energy harvester (CTEH) is the instable output induced by the wide-range variations of the current in transmission lines. In this work, a novel CTEH capable of generating a stable output is demonstrated by using a core fabricated with saturable magnetic material. The stable output of the CTEH is enabled by the constant voltage-time product in its saturable characteristic. The proposed CTEH is implemented with a resistive load representing the load of electronic devices. When the current in the primary side of the CTEH's increases from 1 to 1000 A, the maximum power on the load can reach about 0.5 W, demonstrating the feasibility of using the CTEH with the saturable magnetic core as a quasi-stable power supply.

Introduction: The rapid increase in the number of industrial wireless sensor nodes demands new power supply options. For the in-situ monitoring of high-voltage transmission lines, common power supplies, such as solar energy [1], wind energy, battery or laser energy [2], are known to have insufficient stability and sustainability. In comparison, it is more reasonable to generate power from the current transmitted in the highvoltage transmission lines, namely the current transformer (CT) principle. However, the output power of CT is often either too low or saturated, as a result of the wide range of transmitted current between a few amperes to thousands of amperes. The low output power may not be enough to supply energy to the electronic devices, while the surplus power must be consumed in order to avoid the damage of electronics devices. Especially, when the short-term surge current presents in the transmission lines, the CT's magnetic core might be saturated, overheated and even burned. One way to desaturate the magnetic core under high current is to use a bleeder circuit on the CT's secondary side [3], for example, a stable power output of 0.65 W is realized when the CT primary side current is in the range of 17 to 500 A. Furthermore, CT with multiple secondary side taps and short-circuiting taps implemented with electronic switches is shown to be effective in avoiding the saturation of CT magnetic core in a wide current range and supply sufficient energy [4]. Similarly, a desaturation controller [5] might be used to harvest energy from power line, where energy harvesting efficiency is improved by 13.7%. In addition, a traditional CT might be implemented with an air gap cutting structure in the CT magnetic core [6], enabling 10-W output power with transmitted current between 100 and 1000 A. As an alternative approach, a capacitance compensation circuit can be utilized to desaturate the CT magnetic core and harvest energy effectively [7]. The CT energy harvester, after optimizing the parameters, can increase the output power and work in a wide range of current in the transmission line. In fact, for a CT with predefined physical parameters, its maximum harvesting power is directly proportional to the square of the primary current [8]. Therefore, with the increase in the transmitted current, the energy harvested by the CT's secondary side will increase correspondingly.

Despite the excellent energy-harvesting capability in the unsaturated state, most of the CT energy harvesters can yet not harvest energy effectively when its core is saturated. In addition, it is not possible to avoid the damage caused by the surge of large current in the transmission line. Consequently, these harvesters may suffer from serious heating problems under the high current condition for a long time.

In this work, a CT energy harvester (CTEH)-based saturable magnetic core is proposed, capable of generate stable output power in the large current range of the transmission line. The main novelty of this work is the CT's easiness of saturation and high capability of power generation enabled by the extremely high relative permeability of the magnetic

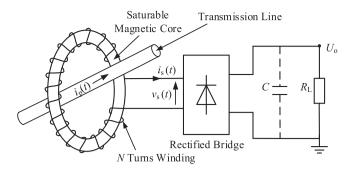


Fig. 1 CTEH circuit. CTEH, current transformer energy harvester.

core material. Meanwhile, the narrow magnetic hysteresis of the material made it possible to generate the much low loss. The working principle, design, and first characterization results of the CTEH are presented in this paper.

Operating principle of CTEH: The saturable magnetic material refers to the materials with very high relative permeability (up to 10^6) and small coercive, giving rise to a quasi-rectangular shaped hysteresis loop. The common saturable magnetic materials mainly include the Cobalt-based material, Permalloy and Supermendur. A CTEH processed with those magnetic materials is shown in Figure 1.

Generally, the primary side of CT is the transmission line, equivalent to one turn, and its secondary side is designed to N turns, wound around those ring-shaped magnetic materials. When the primary side current $i_p(t)$ is transmitted, according to Ampere's circuital theorem, the secondary side current $i_s(t)$ is generated and its induced voltage is denoted as $v_s(t)$. Then after rectified bridge and filter C, the output voltage U_o is obtained to supply energy to load R_L . During this period, the hysteresis processing of the saturable core is shown in Figure 2.

In the magnetization curve, the point b is the saturated magnetic flux density denoted as $B_{\rm s}$, and the corresponding field intensity is $H_{\rm s}$. The remanence is denoted as $B_{\rm r}$ (shown in point a in the figure), and the coercive force is denoted as $H_{\rm r}$. Taking the quasi-rectangular shaped hysteresis loop of Cobalt-based as an example, the saturated magnetic flux density of point c is almost equal to that of point b, which is about 0.55 Tesla, and the rate of $B_{\rm r}$ and $B_{\rm s}$ is above 0.85.

When $i_p(t)$ increases from zero to the value of i_{t1} , the magnetization changes from the point a' to the point b on the curve. In this process, the flux density B is changed from $-B_r$ to B_s , so the induction voltage $v_s(t)$ is generated in the secondary winding of the CTEH. When $i_p(t)$ continues to increase to the value of i_{p-pk} , the magnetization curve increases from points b to c. In this process, the magnetic core remains saturated, and the variation of magnetic flux density from points b to c is zero. As a result, $v_s(t)$ is decreased to zero. Furthermore, when $i_p(t)$ decreases from i_{p-pk} to zero, the magnetization curve moves from points c to a. The variation of magnetic flux density at these two points is equal to (B_s-B_r) , less than 0.15, and then $v_s(t)$ should be small, approximately zero. As the negative half cycle of the magnetization begins, the magnetic core is released from the saturation state and a negative voltage is induced. The shaded area in Figure 2 represents the period of time when $v_s(t)$ can be generated in the secondary winding of the CTEH.

According to Ampere's circuital theorem, the magnetic field intensity H is $H = k \times i_p$, where k is determined by the ratio of the number of the winding turns to the length of the effective magnetic path. When H is noted as H_s , i_p is defined as the saturated current i_{t1} . When the magnetic core of CT is determined, H_s is the fixed value and so is i_{t1} . As shown in Figure 2, the variation of current i_{t1} is trivial regardless the change of value of $i_p(t)$. Therefore, the saturated time t_1 can be obtained.

 $i_{\rm p}(t)$ is expressed as $i_{\rm p}(t)=i_{\rm p.pk}\times\sin(2\pi f\times t)$, and f is the line frequency. When the current value is $i_{\rm t1}$, the corresponding time $t_{\rm 1}$ can be expressed as follows:

$$t_1 = \frac{1}{\omega} \arcsin\left(\frac{i_{t1}}{i_{p-pk}}\right) \tag{1}$$

¹Xi'an Jiaotong University, Xi'an City, China

²Politecnico di Torino, Corso Duca degli Abruzzi, Torino, Italy

[™]Email: Caoja@mail.xjtu.edu.cn

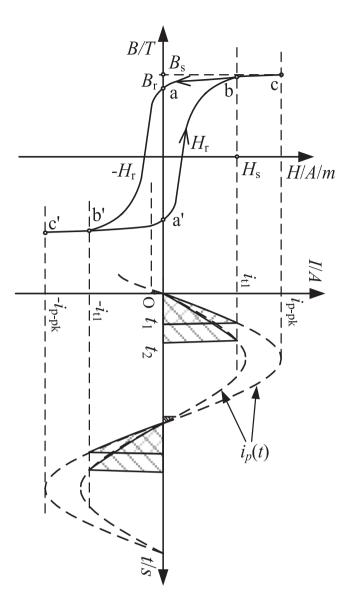


Fig. 2 Operating principle of CTEH

It can be concluded from Equation (1) that t_1 decreases with the increase of $i_p(t)$. And with the decrease in $i_p(t)$, the saturated time increases to t_2 shown as Figure 2.

The secondary side induces voltage $v_s(t)$ of CTEH as follows:

$$v_{\rm s}(t) = -N \times \Delta B \times S/\Delta t \tag{2}$$

For the CTEH with the saturable magnetic core, the value Δt is the time when $\nu_s(t)$ is generated before the magnetic core is saturated and equal to t_1 or t_2 in Figure 2. ΔB equal to $2B_s$ is a fixed value, that is, 1.1 Tesla for the Cobalt-based material. N, the CT's secondary side turns N_s , and S, the CT's magnetic core sectional area, are both defined value.

The voltage second product Λ is defined as: $\Lambda = v_s(t) \times \Delta t$. That is

$$\Lambda = v_s(t) \times \Delta t = -N \times 2B_s \times S \tag{3}$$

Therefore, Λ can be fixed. Furthermore, if T is the period for the transmission line current, the output average voltage U_0 in Figure 1 is equal to $2\Lambda/T$. That means, the CTEH can supply stable output voltage U_0 for electronic devices, independent of the variation of the CT primary side current $i_p(t)$. That is

$$U_0 = -4N \times B_s \times S/T \tag{4}$$

Materials and methods: According to the scheme illustrated in Figure 1, the prototype for the experiment and verification is built as shown in Figure 3. The CTEH is a ring-shaped saturable core winded with coils,

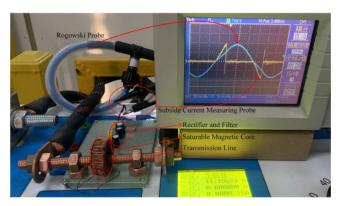


Fig. 3 CTEH prototype for experiment and verification

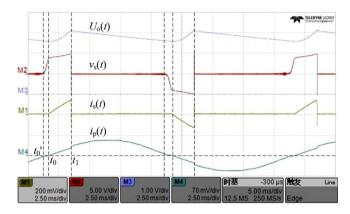


Fig. 4 Voltage and current waveforms of CT primary side and secondary side

and it is installed around the transmission line. The CTEH magnetic core is fabricated with a Cobalt-based material 6025 Z from VAC Company, with the model number E4030W543. The transmission line current ranged from 1 to 1000 A and is generated by the current source of model SDDL-3000A. Observing and recording waveforms are achieved by the oscilloscope of model LeCroy's HDO4054. The voltage second product of the magnetic core is a constant and will be integrated by the oscilloscope.

The CTEH primary side has one turn while the secondary side has 90 turns. $R_{\rm L}$ is 220 Ω and C is 220 μ F.

The voltage and current waveforms of the CTEH primary and the secondary are shown in Figure 4. The ratio of $i_{\rm p}(t)$ is $1\,{\rm V}/500\,{\rm A}$ according to Rogowski probe calibration, and the ratio of $i_{\rm s}(t)$ is $1\,{\rm V}/1\,{\rm A}$ measured by connecting 1 Ohm resistance in series. When the transmission line current $i_{\rm p}(t)$ is about 25 A excited by the current source, the CT's secondary side peak voltage $v_{\rm s}(t)$ is about 5 V, while the current $i_{\rm s}(t)$ is rectified and fed through a constant load $R_{\rm L}$ connected to the capacitor C in Figure 1. The capacitor C can smooth and filter the output voltage $U_{\rm o}$, then output power is $U_{\rm o}^2/R_{\rm L}$.

Results and discussions: In Figure 4, between time t_0 and time t_1 , part of $i_p(t)$ is transformed to $i_s(t)$ by CTEH. When $i_s(t)$ charges up the capacitor C, the voltage $v_s(t)$ is generated and rectified, forming the output voltage U_o . The time period from t_0' to t_0 is corresponding to the magnetization process from point b' to point a' in Figure 2. The variation of magnetic field ΔB ($= B_s - B_r$) is so small that the induced voltage $v_s(t)$ is very low and the $i_s(t)$ is almost negligible.

In order to investigate the CTEH capacity in the range of the large current variation, the Cobalt-based magnetic core is replaced by a Supermendur core in Figure 1, which size is $46 \text{ mm} \times 36 \text{ mm} \times 6.5 \text{ mm}$, and other parameters are not changed. When the current $i_p(t)$ is varied from 1 to 1000 A, the experimental results are shown in Figure 5.

When the CTEH is loaded with a pure resistive load $R_{\rm L}$ without the capacitor C, the output voltage $U_{\rm o}$ (mV) (left y-axis in Figure 5) can be stably settled down to about 900 mV while the current $i_{\rm p}(t)$ increases from 150 to 1000 A. The continuous and relatively stable output voltage can be described by Equation (4). Subsequently, $R_{\rm L}$ is set to 15 k Ω and

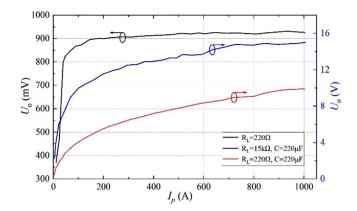


Fig. 5 CTEH with the primary current changing in a large range

connected with the shunt capacitor C to form the filter, the output voltage $U_{\rm o}$ (V) (right y-axis in Figure 5) can be stabilized to a value of around 15 V. When $R_{\rm L}$ is set to 220 Ω as the low power load, $U_{\rm o}$ (right y-axis in Figure 5) can be stabilized to a value of about 10 V, giving rise to a power output of 0.5 W.

Conclusion: This paper proposes a novel CTEH based on a saturable magnetic core, which can generate stable output power in the widerange current of the transmission line. The stable output power of the CTEH is illustrated by the constant voltage—time product with its saturable magnetization characteristic and proved by the experiment with the resistive load in the primary side current of the CTEH's increasing from 1 to 1000 A. Also, the maximum power on the load can reach about 0.5 W.

Conflict of interest: The authors declare that they have no known competing financial interests or personal relationships that could have appeared to influence the work reported in this paper.

Funding information: This submission is not supported by funding.

Data availability statementt: The data that supports the findings of this study are available in the supplementary material of this article

© 2022 The Authors. *Electronics Letters* published by John Wiley & Sons Ltd on behalf of The Institution of Engineering and Technology.

This is an open access article under the terms of the Creative Commons Attribution License, which permits use, distribution and reproduction in any medium, provided the original work is properly cited.

Received: 8 May 2022 Accepted: 20 June 2022

doi: 10.1049/ell2.12566

References

- Qian, Z.: Power supply for high voltage circuit of active electronic current transformer. High Voltage Appar. 40(2), 135–138 (2004)
- 2 Zangl, H., Bretterklieber, T., Brasseur, G.: A feasibility study on autonomous online condition monitoring of high-voltage overhead power lines. *IEEE Trans. Instrum. Meas.* 58(5), 1789–1796 (2009). https://doi.org/10.1109/tim.2009.2012943
- 3 Chi, T., Yanzhen, Z., Zijian, T.: Study on energy harvesting of open-close current transformer. In: ICSMD2020, Xi'an, China, 15–17 Oct (2020), pp. 567–571. https://doi.org/10.1109/icsmd50554.2020.9261672
- 4 Gorchakov, A. V., Rashitov, P. A.: High-efficiency power supply for distributed flexible alternative current transmission system devices. In: REEPE, Moscow, Russia, 14–15 March (2019). https://doi.org/10.1109/ reepe.2019.8708843
- 5 Jinhua, W., Jaehoon, K., Dong Sam, H.: Powerline energy harvesting circuit with a desaturation controller for a magnetic core. In: MWSCAS, Lansing, MI, USA, 9–11 Aug (2021) pp. 220–223. https://doi.org/10.1109/mwscas47672.2021.9531890
- 6 Wen, Z., Zhengyang, L., Qinqing, H., Yi, J., Zihan, C.: Design of magnetic cores for current transformer energy harvesting devices. In: APPEEC, Macau, China, 1–4 Dec (2019), p. 5. https://doi.org/10.1109/ appeec45492.2019.8994809
- 7 Wang, J., Chen, W.: Output characteristics analysis of energy harvesting current transformer. *IEEE Sens. J.* 21(20), 22595–22602 (2021). https://doi.org/10.1109/jsen.2021.3107864
- 8 Li, P.: The influence factors of CT output performance for power transmission cables. *Electomech. Components* 10, 41(5), 53–60 (2021)